JVR
Journal of
Vascular Research

Methods in Vascular Biology

J Vasc Res 2023;60:1–11
DOI: 10.1159/000529115

Received: May 25, 2022
Accepted: December 12, 2022
Published online: March 7, 2023

Validation of an ex vivo Flow Model Including Magnetic Resonance Imaging to Study the Effects of Endovascular Treatments on the Arterial Wall

Raúl Devia Rodriguez[a] Eline Huizing[a, b] Çağdaş Ünlü[b] Frank F.J. Simonis[c] Reinoud P.H. Bokkers[d] Jean-Paul P.M. de Vries[a] Richte C.L. Schuurmann[a] Dalibor Nakladal[e] Hendrik Buikema[e] Jan-Luuk Hillebrands[f] Henri G.D. Leuvenink[g]

[a]Division of Vascular Surgery, Department of Surgery, University Medical Centre Groningen, University of Groningen, Groningen, The Netherlands; [b]Department of Surgery, Northwest Clinics, Alkmaar, The Netherlands; [c]Department of Science and Technology, TechMed Centre, University of Twente, Enschede, The Netherlands; [d]Department of Radiology, Medical Imaging Center, University Medical Centre Groningen, University of Groningen, Groningen, The Netherlands; [e]Department of Clinical Pharmacy and Pharmacology, University Medical Centre Groningen, University of Groningen, Groningen, The Netherlands; [f]Division of Pathology, Department of Pathology and Medical Biology, University Medical Centre Groningen, University of Groningen, Groningen, The Netherlands; [g]Surgical Research Laboratory, Department of Surgery, University Medical Centre Groningen, University of Groningen, Groningen, The Netherlands

Keywords
Percutaneous transluminal angioplasty · Benchtop flow model · Ex vivo porcine arterial perfusion · Endovascular treatment/therapy · Magnetic resonance imaging

Abstract
Endovascular revascularization is the preferred treatment for peripheral arterial disease. Restenosis often occurs as a response to procedure-induced arterial damage. Reducing vascular injury during endovascular revascularization may improve its success rate. This study developed and validated an ex vivo flow model using porcine iliac arteries, obtained from a local abattoir. Twenty arteries (of 10 pigs) were equally allocated to two groups: a mock-treated control group and an endovascular intervention group. Arteries of both groups were perfused with porcine blood for 9 min, including 3 min of balloon angioplasty in the intervention group. Vessel injury was assessed by calculating the presence of endothelial cell denudation, vasomotor function, and histopathological analysis. MR imaging displayed balloon positioning and inflation. Endothelial cell staining showed 76% of denudation after ballooning compared to 6% in the control group ($p < 0.001$). This was confirmed by histopathological analysis, showing a significantly reduced endothelial nuclei count after ballooning compared to the controls (median: 22 vs. 37 nuclei/mm, $p = 0.022$). In the intervention group, vasoconstriction and endothelium-dependent relaxation were significantly reduced ($p < 0.05$).We present an ex vivo flow model to test the effects of endovascular therapy on the

Raúl Devia Rodriguez and Eline Huizing contributed equally to this work and share the first authorship of this research.
Jan-Luuk Hillebrands and Henri G.D. Leuvenink contributed equally to this work and share the last authorship of this research.
Hendrik Buikema died on July 2, 2021.

Karger@karger.com
www.karger.com/jvr

Correspondence to:
Raúl Devia Rodriguez, r.devia.rodriguez@umcg.nl

vessel's wall morphology, endothelial denudation, and endothelial-dependent vasomotor function under physiological conditions. Additionally, it allows the future testing of human arterial tissue.

Introduction

Peripheral arterial diseases (PAD) are a major problem for public health, affecting 200 million people worldwide [1, 2]. Endovascular revascularization is one of the preferred treatments for PAD [3]. The mid- and long-term results of endovascular revascularization are, however, varying in patients due to the severity of primary disease and the development of restenosis [4, 5].

Moreover, there is compelling evidence that acute endothelial damage caused by revascularization is related to the late-onset occurrence of restenosis [6, 7]. Hence, strategies for preventing endothelial damage can potentially improve patients' outcomes. For these reasons, endovascular devices are the target for technological development to improve success rates [8]. However, the novel modalities and techniques are most commonly tested in animal studies, which is not the preferred choice. Instead, ex vivo models using animal tissue from abattoirs can be a promising alternative. There is a need for a validated ex vivo model, with a standardized physiological environment including independent control of pressure, resistance, flow, real-time imaging of vessel deformation, and the possibility to accurately assess the vascular function. Furthermore, the use of material from animals for human consumption avoids the use of dedicated laboratory animals and is well in accord with the replacement, reduction, and refinement principles of the EU directive 2010/63/EU [9].

Previous ex vivo flow models for evaluating endovascular treatments for PAD lack real-time imaging [10, 11] and have limited replication of physiological conditions including the use of blood [10, 12]. This is an important aspect as the perfusate viscosity has an impact on the wall shear stress, which is associated with vessel wall remodeling and thrombus formation [13]. In addition, certain blood cells, such as activated monocytes and granulocytes, play a role in developing intimal hyperplasia [14]. The aim of this study was to develop and validate an ex vivo flow model to study the effects of endovascular therapy on the arterial wall in a standardized setting under physiological conditions and MR monitoring.

Materials and Methods

Tissue Harvest and Preparation

Arteries were harvested from 6-month-old female Yorkshire pigs from the local abattoir (Kroon Vlees, Groningen, The Netherlands). All pigs were slaughtered according to the laws and principles of the Dutch Food and Consumer Product Safety Authority. Blood was collected directly after the pigs were slaughtered, and 25,000 IU/L of heparin (LEO Pharma A/S, Ballerup, Denmark) was added to prevent clotting. The distal section of the descending aorta to the proximal part of the superficial femoral arteries was dissected and immediately placed in cold Ringer's lactate (RL; Baxter BV, Utrecht, The Netherlands). The removal of large segments of fat and surrounding tissues was performed on a bed of ice under hypothermic conditions (0–4°C). The cleaned arterial segment was transported to the laboratory in RL solution in a polystyrene cooling box filled with ice. Subsequently, the artery was cleaned from remaining adipose tissue under hypothermic conditions, the side branches were sutured (Silkam black 6/0, B. Braun, Melsungen, Germany), and the artery was tied to polyamide tube couplings to establish a connection to the perfusion setup.

The Animal Research Ethics Committee of the Faculty of Medical Sciences of the University of Groningen waived the requirement for approval, considering that the iliac arteries were obtained from abattoir waste. All tests were performed in accordance with the European regulations and directives on the protection of animals for scientific purposes [9].

Perfusion Setup

The ex vivo flow model consisted of an acrylic pipe perfusion chamber in which the artery was mounted, a perfusate reservoir, a centrifugal pump (Deltastream DP3, MEDOS Medizintechnik AG, Stolberg, Germany), a hollow fiber membrane oxygenator (HILITE 800LT, MEDOS Medizintechnik AG, Stolberg, Germany) connected to carbogen (5% CO_2 and 95% O_2 with 500 mL/min) and a water bath. A Y-connector allowed placement of a sheath as well as the insertion of the angioplasty balloon (shown in Fig. 1c). A flow sensor (ME7PXL clamp, Transonic Systems Inc., Ithaca, USA), pressure sensor (TruWave disposable pressure transducer, Edwards Lifesciences, Irvine, USA), and pump were connected to the SophistiKate 2.0 (Groningen, The Netherlands) hardware system, which could be controlled by the accompanying software on the laptop. The portable MRI system (Training MRI system, Pure Devices GmbH, Rimpar, Germany) has a cylindrical bore that is opened at both sides to allow passage of the perfusion chamber. A closed circulation was created by connecting the components with silicone tubing (shown in Fig. 1).

Setting up the Flow Model for Experiments

One liter of porcine heparinized blood was enriched with 1,000 mg/200 mg amoxicillin/clavulanate (Sandoz BV, Almere, The Netherlands), 10 mL 8.4% sodium bicarbonate (B. Braun Melsungen AG, Melsungen, Germany), 10 mL glucose 5% (Baxter BV), and 20 mg/L dexamethasone (Centrafarm, Etten-Leur, The Netherlands). The enriched blood was perfused for 5 min before the artery was attached in order to obtain normothermic conditions and oxygenate the solution. The artery was attached to the tubing with the flow direction matching the in vivo route and was gently moved inside the perfusion chamber.

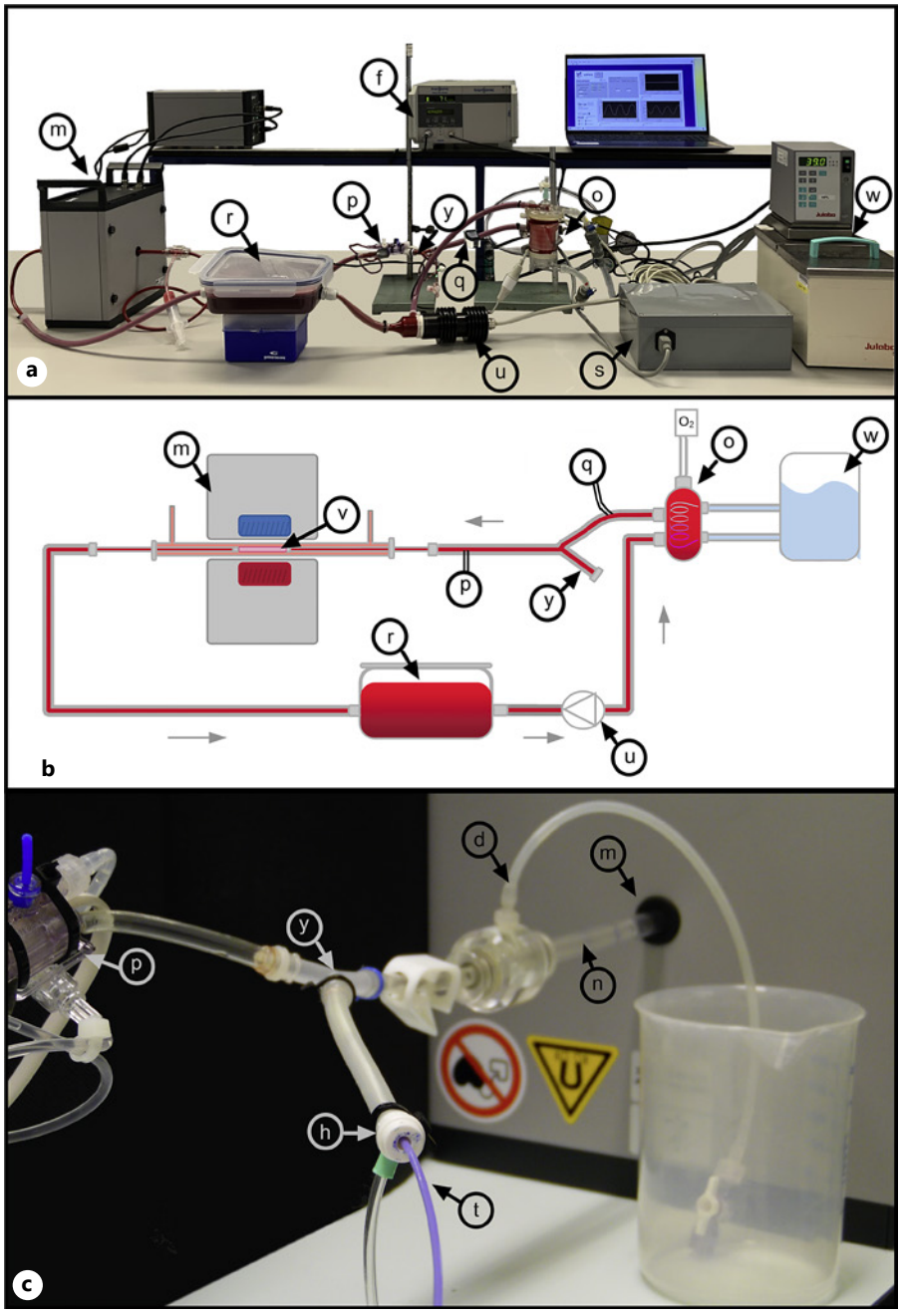

Fig. 1. Overview of model setup. **a** Photograph of setup showing the MRI system. **b** Schematic view of perfusion system. **c** Picture of the Y-connector with the sheath and balloon inserted. d: DMEM insertion place. f: Flow meter. h: Sheath. m: Tabletop MRI system. n: Perfusion chamber. o: Oxygenator. p: Pressure sensor. q: Flow sensor. r: Perfusate reservoir. s: SophistiKate system hardware. t: Balloon catheter. u: Pump. v: Vessel. w: Water bath. y: Y-connector angioplasty port. DMEM, Dulbecco's Modified Eagle Medium.

Custom-made connectors were applied to close the perfusion chamber, which was filled with Dulbecco's Modified Eagle Medium (BioWhittaker, with 4.5 g/L glucose and L-glutamine, Lonza, Basel, Switzerland). The centrifugal pump was pressure controlled and set to a mean arterial pressure of 40 mm Hg to match the circumferential stretch ratio to the in vivo condition [15]. Tubing between the perfusate bath and the artery was compressed using a Hoffman tube compressor to reach an average flow of 70 mL/min to minimize the mural shear stress [16]. Nevertheless, the model and wall shear stress were not calculated. A 6-Fr sheath (BRITE TIP, Cordis, Miami Lakes, FL, USA) was introduced in the Y-catheter for introduction of a guidewire and balloon.

Experimental Design

From 10 pigs, 10 left and 10 right external iliac arteries were used for the experiments, with one vessel randomly allocated to the control group and the contralateral vessel to the intervention group. Arteries in the control group were perfused for 9 min (with controlled pressure of 40 mm Hg and a starting flow of 70 mL/min) without ballooning (shown in Fig. 2). In the intervention group,

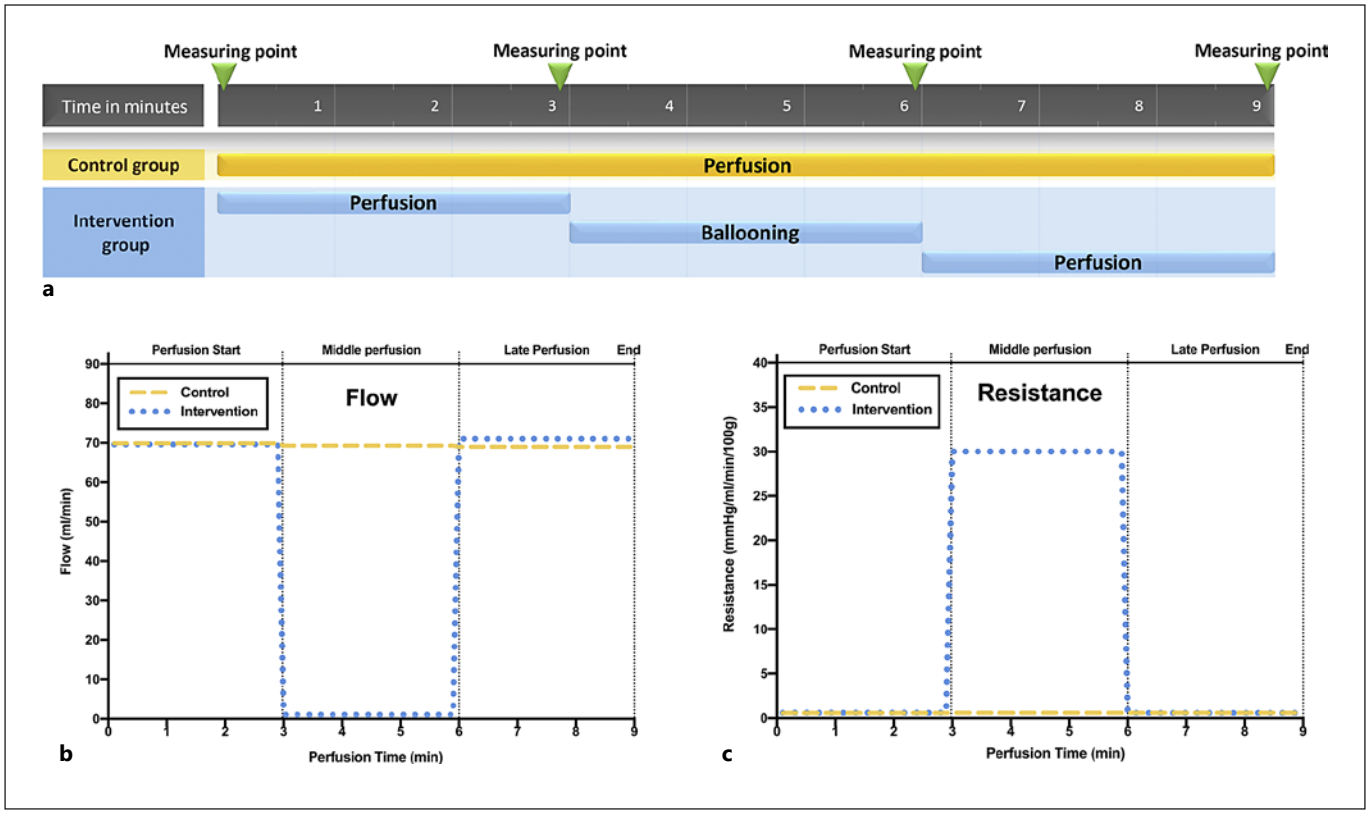

Fig. 2. Summary of the procedure including measurement points. Perfusion was pressure controlled and set at 40 mm Hg with a flow of 70 mL/min. The pressure-controlled pump was not shut down during ballooning. Flow and pressure were measured at 4 time points during perfusion, and resistance was calculated from these variables. **a** Perfusion timeline. **b** Perfusion average flow in the control and intervention group. **c** Perfusion average resistance in the control and intervention groups calculated by the perfusion system applying Ohm's law.

the arteries were perfused for a total of 9 min under the same conditions. After 3 min of perfusion, a guidewire (Amplatz, Cook Medical, Bloomington, IN, USA) was inserted followed by an 8 mm × 2 cm balloon (Advance 35 LP, Cook Medical). Following the balloon placement, the guidewire was withdrawn to remove any metal material that could interfere with MRI. The balloon was inflated (Encore™ 26 inflator, Boston Scientific, Marlborough, MA, USA) to a pressure of 8 atm according to the instructions for use. During inflation, MR images were acquired to evaluate balloon position and vessel deformation as proof-of-concept. After 3 min of inflation, the balloon was deflated, withdrawn from the model, and perfusion was continued for another 3 min. Flow and pressure were measured at 4 time points during pressurization (at baseline, 3 min, 6 min, and 9 min of perfusion, shown in Fig. 2); resistance was calculated from these variables following Ohm's law. To evaluate the effects of ballooning, the artery was detached from the model and prepared for assessment of macroscopic vascular damage, histopathology, and vascular functionality tests.

MR Imaging

MR imaging was performed with a 0.45T portable MRI scanner (Pure Devices, Rimpar, Germany) with a 1 cm diameter bore. Two-dimensional (2D) and three-dimensional (3D) MR scans were acquired transversally and longitudinally to the vessel by means of a fast low angle shot sequence with parameters shown in Table 1. Contrast fluid (Gadoteric acid, Dotarem, Guerbet, Villepinte, France) was applied to the blood (1 mL/L) and to the Dulbecco's Modified Eagle Medium (0.1 mL/15 mL) to optimize imaging when the vessel wall was not clearly visible. In plane, spatial resolution was 0.25 × 0.25 mm^2 and 0.156 × 0.156 mm^2 for the 2D and 3D images, respectively.

Macroscopic Endothelial Damage

A total of 10 arteries (5 per group) were assessed for macroscopic and microscopic endothelial damage. After perfusion, the artery was detached from the model and rinsed with 10 mL NaCl 0.9% to remove any remaining blood. The artery was flushed with 5 mL 0.125% Evans blue (EB; Sigma-Aldrich, Saint Louis, USA) into the vessel lumen [17], followed by rinsing with 10 mL NaCl. Finally, the arteries were cut longitudinally and pinned on a dissection board for visualization of endothelial denuded areas (colored blue with EB staining) and subsequent photography [18].

Photographs were taken using a digital photo camera (WB1100F, Samsung, Seoul, South Korea) in a portable photo studio (Puluz, Shenzhen, China) with an indirect light LED ring. The same manual settings were used for every image, and the white balance was constant for all acquisitions.

Table 1. MRI parameters and settings used for 2D and 3D imaging

Sequence parameters	2D FLASH	3D FLASH
TE/TR, ms	9/100	9/100
Flip angle, °	68.4	68.5
Phase oversampling, %	400	200
Acquired resolution	0.156×0.156 mm^2	$0.25 \times 0.25 \times 0.625$ mm^3
Slice thickness	2 mm	–
Field of view	10×10 mm^2	$10 \times 10 \times 10$ mm^3
Number of signal averaging	4	4
Acquisition time	1′46″	8′6″

TE, echo time; TR, repetition time; FLASH, fast low angle shot.

FIJI (ImageJ Version 2.1.0 Open Source) was used to calculate the blue-stained (denuded) area in each artery [19]. All photos were cropped digitally for image processing, delimiting the 2.5 cm ballooned segment on every artery subjected to ballooning treatment; likewise, 2.5 cm of the middle part in the control arteries was delimited, with the exclusion of side branches. Similarly, the vessel lumen was segmented using the polygon selection feature, and the total pixels of the vessel lumen were measured.

Determining the Denuded (Blue) Area

The pictures were normalized for brightness and contrast by controlling the display ranges' lower and upper limits; the color balance feature was set to a maximum of 50 and a minimum of 207. Likewise, the color segmentation threshold tool with YUV (luminance, blue, and red projection) was used to select the blue-stained area, and a threshold limit of 183 was determined. Finally, the number of the blue selected pixels was measured and divided by the total pixels of the surface area to calculate the percentage of denuded area [20].

Histopathology

After the assessment of endothelial damage with EB, two specimens of 2 mm per artery were cut. Specimens of arteries in the intervention group were taken from the middle and distal parts of the ballooned area. Likewise, specimens of the middle segments were obtained from arteries in the control group. The specimens were immersion-fixed in 10% neutral buffered formalin for at least 24 h followed by paraffin embedding, sectioning (3 μm cross-sections), histochemistry (hematoxylin and eosin, Verhoeff [EVG]), and immunohistochemistry (ETS-related gene [ERG], rabbit monoclonal antibody clone EPR3864, endothelial cell-specific transcription factor). Following (immuno)histochemistry (Ventana BenchMark Ultra, Roche Diagnostics, Almere, Netherlands), sections were digitalized using a NanoZoomer slidescanner (Hamamatsu Photonics, Hamamatsu, Japan) followed by computerized morphometric analysis using NDP.view2 viewer software (Hamamatsu Photonics).

The degree of endothelial denudation was quantified by counting the endothelial nuclei as seen in ERG-stained sections and divided by the total length of the surface lining. The thickness of the smooth muscle layer was measured at 6 different segments of the artery in the H&E-stained sections and averaged. Assessments of nuclei and smooth muscle layer were performed independently by two authors (E.H. and R.D.R.), who were blinded to the treatment group during the assessment.

Vasomotor Function

In an additional series of experiments with 10 arteries (5 per group from 5 pigs), the effects of ballooning on vascular function were assessed using potassium chloride (KCl; P3911, Sigma-Aldrich, Zwijndrecht, The Netherlands), phenylephrine (PE; P6126, Sigma-Aldrich), calcium ionophore (CI; C7522, Sigma-Aldrich), and sodium nitroprusside (SNP; 71778, Sigma-Aldrich). After perfusion, the arteries were cut into 4 equal-sized rings (3 mm long segments) from the ballooned segment (intervention group) and middle segment (control group). Rings were mounted in organ baths for the measurement of isotonic displacement as described previously (n = 40 arterial rings from 10 arteries) [21]. Arterial rings were washed several times with Krebs buffer and allowed to equilibrate for a period of 60 min under 1.4 g of resting tension. Thereafter, the rings were assessed for contractile function by inducing 2 subsequent constrictions with KCl (60 mM), a receptor-independent vasoconstrictor, with washout and stabilization in between. Rings that failed to produce a threshold displacement of 150 μm as a response to KCl were excluded (n = 4 arterial rings).

After washout and stabilization, arterial rings were constricted with cumulative doses of PE (30 nM–1 μM), a selective α1-adrenergic receptor agonist. This was followed by stimulation of the endothelium with cumulative doses of CI (6 nM–6 μM) to induce a receptor-independent endothelium-mediated relaxation response [6, 22, 23]. After the last dose of CI, a direct nitric oxide donor SNP was given at a single high dose (100 μM) to induce (maximal) endothelial-independent relaxation and demonstrate capacity of the smooth muscle to per se dilate in response to nitric oxide in these conditions. Rings that did not produce a relaxation response to SNP of at least 80% of the PE constriction were excluded from analysis (n = 1 arterial ring).

Statistical Analysis

Statistical analyses were performed using SPSS, version 27.0 (SPSS Inc., Chicago, IL, USA). Values in vascular response figures are displayed as mean ± SEM of n independent experiments. Vascular relaxation responses are normalized as percentage ranging from the contractile response to the highest PE concentration (100% contraction). Other values are displayed as median ± interquartile range (IQR). Differences between groups were assessed using the Mann-Whitney U test. Statistical significance was defined as $p < 0.05$.

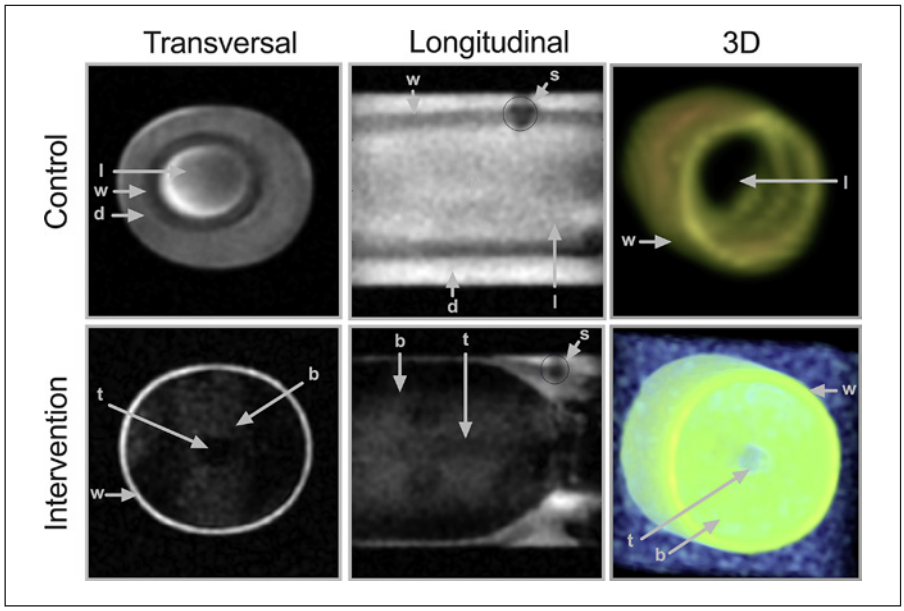

Fig. 3. 2D and 3D MR images in longitudinal and transversal direction of arteries in both groups. The upper row represents an artery in the control group during perfusion. The lower row represents an artery in the intervention group, in which balloon placement and arterial morphology were observed. Stretching of the artery and a thinner arterial wall are clearly visible during the endovascular procedure. A sutured side branch was observed in the longitudinal images, and a similar thinner arterial wall is observed in the balloon-inflated segment of the artery. In the 3D images, the artery is displayed in yellow, the balloon in green, and the air in blue. b: Inflated balloon. d: DMEM. l: Vessel lumen. t: Balloon angioplasty catheter. s: Sutured side branch. w: Vessel wall. DMEM, Dulbecco's Modified Eagle Medium.

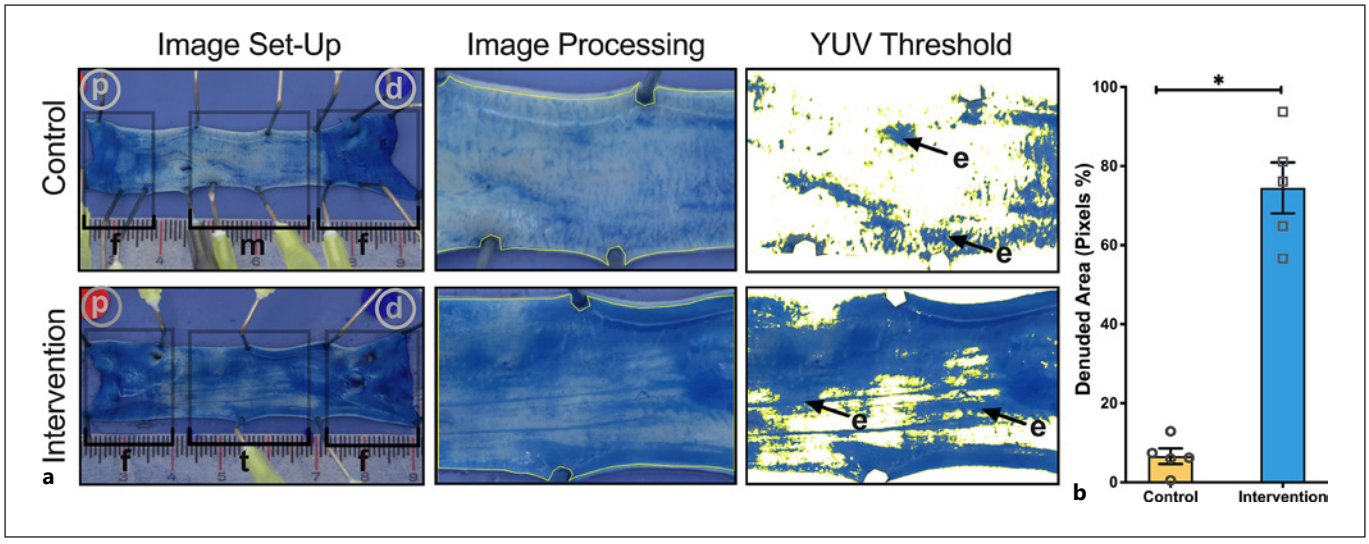

Fig. 4. EB staining reveals increased endothelial denudation upon intervention (ballooning). Blue-colored areas demonstrate loss of endothelial cells. **a** Process of EB staining and analysis per group. **b** Mean (±SEM) percentage of EB staining of the mid- or ballooned part for the control and treatment group, respectively (n = 5 per group). p: Proximal arterial side. d: Distal arterial side. f: Fitting arterial attachment space, showing severe endothelial damage. m: (Sham-treated) mid-arterial part. t: Ballooned arterial part. e: Denuded areas identified by EB positivity, indicating endothelial injury. (*) Significant difference of $p < 0.001$, calculated using Mann-Whitney U test.

Results

The median length of arteries in the intervention and control groups was 7.0 cm (IQR; 6.4–7.1 cm) and 7.0 cm (IQR; 6.0–7.1 cm), respectively ($p = 0.912$). Similarly, the diameter of the arteries had a median of 4.5 mm (IQR; 4.0–5.3 mm) in the intervention group and 4.0 mm (IQR; 4.0–4.6 mm) in the control group ($p = 0.280$).

Perfusion Behavior

The recorded parameters of flow and resistance are shown in Figure 2b and c.

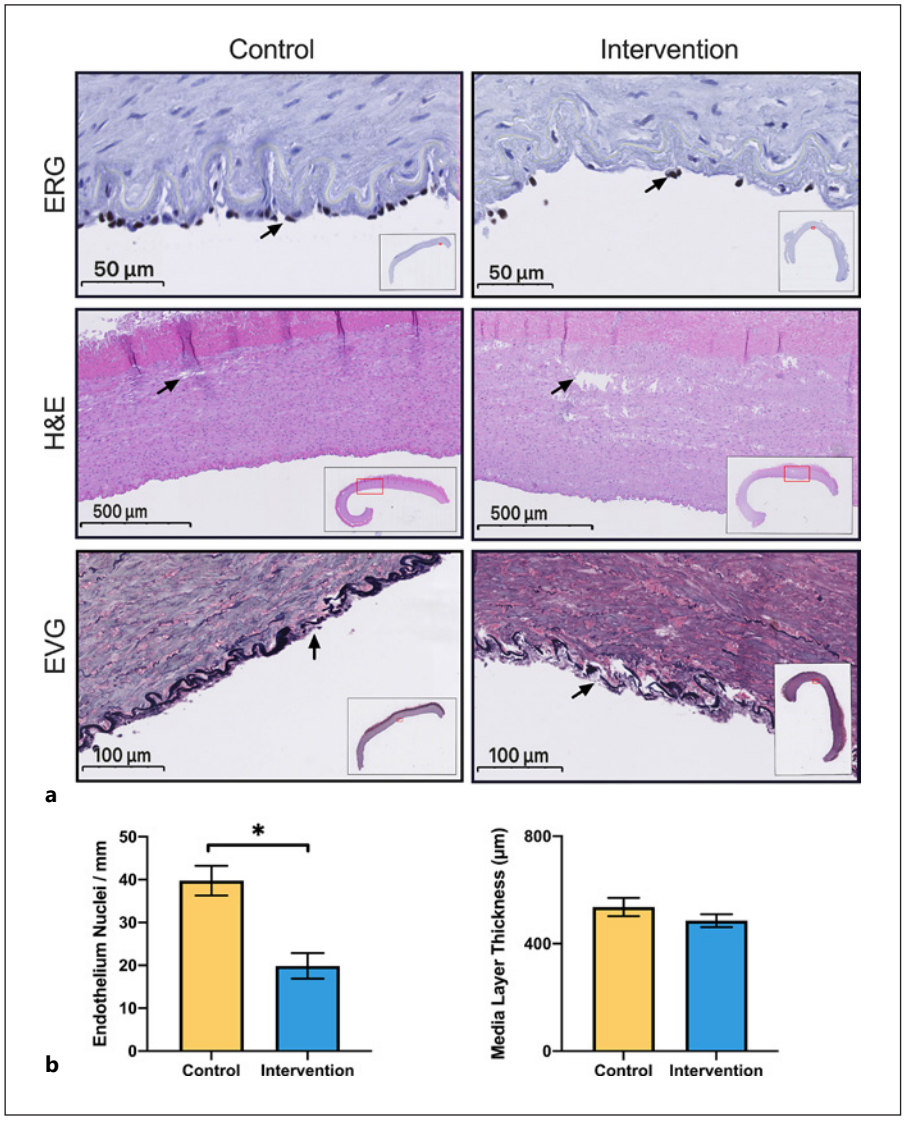

Fig. 5. a Histopathology staining results and analysis. Images of ERG, H&E, and EVG stained sections per group. The ERG-stained section in the control group shows more endothelial nuclei (indicated by the arrow) when compared to the section of the intervention group. In some of the H&E-stained slices, disruptions in the medial layer were observed (indicated by the arrow). In the intervention group, the disruptions were larger and more severe. Disruptions of the internal elastic lamina were seen in some of the EVG-stained sections (indicated by the arrow). **b** Graph showing the mean (±SEM) of total nuclei/mm ratio and media thickness per group. (*) Significant difference between the groups in the endothelial nuclei/mm ratio performed in the ERG-stained sections ($p < 0.05$), calculated using Mann-Whitney U test.

MR Imaging

2D and 3D MR imaging clearly visualized balloon positioning and inflation (shown in Fig. 3). The MRI system was not used to perform measurements or quantifications.

Endothelial Denudation after Ballooning

EB staining showed a significantly larger blue-stained (denuded) area in the intervention group (76.1%, IQR; 6.1–87.4%) when compared to the control group (6.2%, IQR; 3.3–10.2%, $p < 0.001$, shown in Fig. 4). Based on the ERG staining, significantly fewer endothelial nuclei were observed in the intervention group (22 nuclei/mm, IQR; 11–28 nuclei/mm) when compared to the control group (37 nuclei/mm, IQR; 32–44 nuclei/mm, $p = 0.022$). Furthermore, disruptions in the medial layer were observed in both groups. The area of the disruptions was significantly larger in the intervention group when compared to the control group (1,668 µm^2, IQR; 895–9,679 µm^2 vs. 372 µm^2, IQR; 292–799, respectively; $p = 0.018$). Inner elastic lamina fragmentation was seen in both groups but was more extensive in the intervention group (935 µm vs. 106 µm fragmented length, shown in Fig. 5). The thickness of the medial layer was not significantly different between the intervention and control groups, with a median thickness of 476 µm (IQR; 443–580 µm) and 557 µm (IQR; 435–602 µm, respectively ($p = 0.391$).

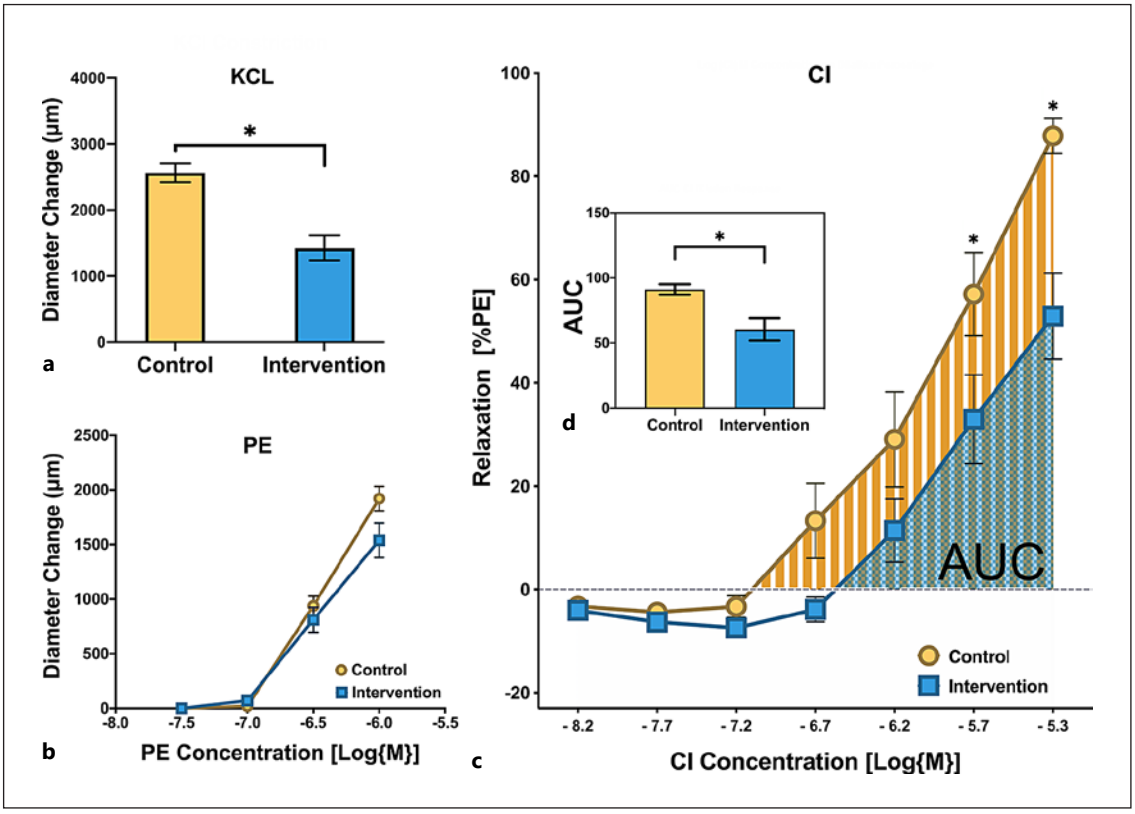

Fig. 6. Vascular response analysis. **a** Diameter change in response to second dose of potassium chloride (KCl). **b** Constriction response to cumulative phenylephrine (PE) concentrations. **c** Endothelium-dependent relaxation response to cumulative calcium ionophore (CI) concentrations. **d** AUC summary of CI relaxation responses. (*) Significant difference between the intervention and control groups ($p < 0.05$), calculated using Mann-Whitney U test. Data from 10 experiments ($n = 35$ arterial rings, from 10 arteries).

Vasomotor Function

The diameter change response to a single dose of KCl was significantly lower in the intervention group (1,452 µm, IQR; 790–2,031 µm) when compared to the control group (2,490 µm, IQR; 2,199–3,182 µm, $p < 0.001$, shown in Fig. 6a). Responses to PE (1 µM) were not different between the groups ($p = 0.200$), with a median diameter change of 1,571 µm (IQR; 2,045–1,064 µm) and 1,863 µm (IQR; 2,049–1,550 µm) in the intervention and control groups, respectively. The subsequent endothelium-dependent relaxation in response to CI at 6 µM showed a reduced median relaxation of 51% (IQR; 28–83%) for the intervention group and 94% (IQR; 72–100%) in the control group ($p = 0.001$). Also, when analyzed as area under the curve (AUC), the overall endothelial-dependent relaxation in response to CI was significantly reduced in the intervention group (AUC: 61.4%·Log[M], IQR; 31.5–83.9%·Log[M]) when compared to control arteries (AUC: 98.6%·Log[M], IQR; 76.4–103.7%·Log[M], $p = 0.007$, shown in Fig. 6c, d). Lastly, there was no difference between the control and intervention groups in maximal response to SNP ($p = 0.802$).

Conclusion

Testing new devices and techniques for endovascular treatment of PAD is crucial to improve treatment methods and increase outcome success. Based on the need for an adequate ex vivo flow system that can mimic human physiological conditions, we have developed a state-of-the-art model that is able to assess morphology by MRI and the acute endothelial effects of endovascular therapies using porcine arteries.

Previous experimental models have been developed to investigate the effects of revascularization procedures on

the vascular wall and endothelium such as perfusion bioreactors [24]. These approaches have included machine perfusion flow models, using tissue derived from animal models, human subjects, and/or artificial engineered structures [25, 26]. However, our model is a unique approach developed by adapting tissue transplantation research technology to control perfusion and hemodynamic settings that resemble physiological conditions [27]. Moreover, it gathers essential features used in revascularization procedures, such as imaging, for the adequate positioning of devices and using full blood for perfusion. This study shows that the developed flow model is very suitable for evaluating vascular damage induced by endovascular therapy and its acute effects on vascular function in a standardized setting. But more importantly, the proposed model is a versatile and accessible system that allows further research in the field besides adapting for specific research aims (such as tissue sources, perfusion conditions, and vascular injury evaluation methods).

In the present study, we have shown that there was a significant difference in endothelial presence and functionality between intervention and control arteries when perfused in our ex vivo model. These results demonstrate that short-term treatment effects can be assessed. The need to perfuse arteries in ex vivo models has been demonstrated by a paper by Bardy et al. [28], in which an increase in vascular cell activity was observed in perfused arteries. In addition, blood flow is one of the determinants for vascular wall shear stress, which is associated with the development of atheroma [13]. These findings underline the need to include perfusion in ex vivo models to study the effects of endovascular interventions.

In the present study, a denuded median area of 6% in control arteries was found. This may indicate that ex vivo perfusion itself causes denudation to some extent. Therefore, we evaluated endothelial denudation of non-perfused arteries after cleaning both at the abattoir and at arrival at the lab. No endothelial denudation was found in arteries assessed directly after dissection at the abattoir, with slight denudation (6% denuded area) after transfer to the lab. This denudation may be due to the storage conditions despite the use of Ringer's lactate and a hypothermic environment for transportation. Warm and cold ischemia during harvesting and transport may induce damage to the arteries before they are exposed to the test conditions. We exposed both groups to the same conditions to control this experimental variable.

In the intervention group, we found endothelial denudation, medial layer dissections, and ruptures of the internal elastic lamina. This is in line with previous perfusion ex vivo studies and in vivo animal studies [10, 29], in which the same vascular wall injury was noted along with thinning of the medial layer. In addition, in the ex vivo study [10], significant reduced endothelial nuclei were observed in the intervention group, which was also seen in the present study.

Previous ex vivo and in vivo animal studies described abolished arterial responses to KCl or norepinephrine as a result of the arterial wall impairment after angioplasty [10, 29]. This effect was not confirmed in the current study, but significantly lower arterial constriction to KCl was recorded in the arterial rings subjected to the angioplasty procedure. These results led us to suspect a receptor-independent impairment of vasoconstriction in the vascular smooth muscle cells caused by angioplasty. This finding aligns with the smooth muscle injury ("arterial paralysis") evidenced by Fischell et al. [30] in swine carotid arteries after angioplasty with 8-mm balloons. Furthermore, PE responses representing specific GPCR-mediated vasoconstriction were not significantly affected by balloon angioplasty. Given the limited concentration range of PE studied and the dose-response curves not reaching a plateau, we could not exclude the possibility that angioplasty also affected GPCR-mediated responses. Investigating the effect of angioplasty on specific molecular pathways in vasoconstriction was, however, out of the scope of our study.

In the present study, the endothelium-dependent relaxation responses in the intervention group were reduced by 40% when compared to the control group. This outcome matches our histopathology results, in which 40% less endothelial cells were observed in the intervention group. It is worth noting that histopathology and vascular response tests were not performed in identical arterial rings but separate rings isolated from the same arteries. In any case, the combined results support the validation of the ex vivo model for balloon angioplasty.

During perfusion, MR imaging was used to verify balloon positioning, not to perform measurements or quantifications. As proof-of-concept, additional scans were occasionally performed to assess vessel deformation. This included measuring the inner diameter and vessel wall thickness before and after ballooning. The use of MR imaging opens the opportunity to test elastic recoil of the arterial wall, which is difficult to assess during in vivo interventions. The MRI sequence and the use of contrast fluid should be further investigated to provide robust quality of MR images. On the other hand, the portable tabletop MRI system has a major advantage that it can be used in a laboratory setting; however, the resolution of the MR system is 156–250 microns. Therefore, measuring the

wall thicknesses (about 450–550 microns) may not be very accurate.

Several limitations of the present study should be mentioned. First, we used lesion-free porcine arteries, while the target arteries are human, calcified, and stenotic. For this reason, to account for the difference in compliance between healthy and diseased arteries, an 8 mm balloon was used in this research, following the oversizing approaches proposed by previous research [31]. The advantage of the current setup is that the model can be adjusted for the diameter of the artery, enabling the use of arteries isolated from human amputated legs. By doing so, in future studies, endovascular therapy can be tested in severely calcified human arteries to advance the model even closer to clinical practice. Second, a limitation of this model is that only acute endothelial injury can be assessed, while remodeling is a chronic process. Vascular inflammation, chronic vascular wall remodeling, and intimal fibrin deposition that are associated with restenosis could not be assessed with the current model.

Furthermore, the conditions of ex vivo vessels differ from those in vivo as perivascular tissue support is lacking due to the required dissection of the structures. Hence, the high compliance of the ex vivo vascular tissue presents a limitation of the model, increasing the circumferential stress ratio and producing harm to the endothelium. This issue has previously been addressed by Hamza et al. [15, 32]. They proposed to adapt flow and pressure conditions to correct for this effect, which have been used in our setup by setting a controlled pressure of 40 mm Hg and a continuous flow of 70 mL/min.

Finally, EB dye is a versatile technique widely used in vascular surgery research for its ability to identify denuded areas and endothelial vascular permeability in a relatively large piece of the vessel; however, it is unspecific for endothelial tissue damage [17]. For this matter, more specific endothelial injury evaluation methods were integrated (such as ERG immunohistochemistry and morphometric quantitative analyses), and furthermore, endothelial-dependent vascular function (using myography) was incorporated into this research to corroborate the findings obtained with the EB staining.

Despite the limitations, use of our model contributes to the reduction of the use of animal models for research, thus complying with the replacement, reduction, and refinement guiding principles of animal welfare that are strived for worldwide. Hence, this research shows a successful application of the use of animal byproducts for research in the cardiovascular field and an example of following the European Directive 2010/93/EU.

In conclusion, this study shows that the developed flow model is very suitable to evaluate acute vascular damage induced by endovascular therapy. The model includes all features to assess the effects of endovascular interventions on the vessel wall in a standardized setting under physiological conditions, including controlled flow and pressure. Moreover, it allows the use of calcified human arterial tissue and offers replacement for testing on research animals.

Acknowledgments

This research would like to commemorate Dr. Hendrik Buikema's life, including his academic and personal contributions to our research group. He is remembered and missed. The authors would like to thank Mr. J.J. Zwaagstra and Ms. P.J. Ottens for their support and help during the study. Furthermore, they would like to thank the Pharmacology Department of the UMCG for allowing the use of their setup and equipment for the vascular response tests. Additionally, they would like to express their thanks to Ms. M.L.C. Bulthuis for embedding and processing the histological samples. Further, the authors would like to thank Mr. M. Distler and his company, Pure Devices GmbH, for allowing the use of an MRI scanner in this research project, besides providing constant technical support in the conduction of MR scans. Graphical abstract created with BioRender.com.

Statement of Ethics

This research complies with the European Directive 2010/93/EU. By using animal byproducts for research, this study is waived by the Institutional Animal Care and Use Committee (IACUC). Additionally, the UMCG has been granted an article 2.18 license with regard to the Animal By-Products Regulation with veterinary supervision number 35889.

Conflict of Interest Statement

The authors have no conflicts of interest to declare.

Funding Sources

This research did not receive any specific grant from funding agencies in the public, commercial, or not-for-profit sectors.

Author Contributions

- Raúl Devia Rodriguez and Eline Huizing: conceived and designed the project, conducted experiments, collected data, performed data analysis, and wrote the scientific manuscript.

- Çağdaş Ünlü, Frank Frederikus Jacobus Simonis, Reinoud Pieter Harmen Bokker, Jean-Paul Petrus Maria de Vries, Richte Caspar Leonard Schuurmann, Dalibor Nakladal, Jan-Luuk Hillebrands, Henri Gerrit Derk Leuvenink, and Hendrik Buikema: conceived and designed the project, assisted in data analysis, and revised the manuscript.

Data Availability Statement

All data generated or analyzed during this study are included in this article. Further inquiries can be directed to the corresponding author.

References

1 Spoorendonk JA, Krol M, Alleman C. The burden of amputation in patients with peripheral arterial disease in The Netherlands. J Cardiovasc Surg. 2020;61:435–44.
2 Olinic DM, Spinu M, Olinic M, Homorodean C, Tataru DA, Liew A, et al. Epidemiology of peripheral artery disease in Europe: VAS educational paper. Int Angiol. 2018;37(4):327–34.
3 Bunte MC, Shishehbor MH. Next generation endovascular therapies in peripheral artery disease. Prog Cardiovasc Dis. 2018 Mar;60(6):593–9.
4 Farber A, Eberhardt RT. The current state of critical limb ischemia: a systematic review. JAMA Surg. 2016 Nov;151(11):1070–7.
5 Spreen MI, Martens JM, Knippenberg B, van Dijk LC, de Vries JPPM, Vos JA, et al. Long-term follow-up of the PADI trial: percutaneous transluminal angioplasty versus drug-eluting stents for infrapopliteal lesions in critical limb ischemia. J Am Heart Assoc. 2017 Apr;6(4):e004877.
6 Furchgott RF. Role of endothelium in responses of vascular smooth muscle. Circ Res. 1983;53(5):557–73.
7 Clare J, Ganly J, Bursill CA, Sumer H, Kingshott P, de Haan JB. The mechanisms of restenosis and relevance to next generation stent design. Biomolecules. 2022;12(3):430–26.
8 Waters RE, Terjung RL, Peters KG, Annex BH. Preclinical models of human peripheral arterial occlusive disease: implications for investigation of therapeutic agents. J Appl Physiol. 2004;97(2):773–80.
9 Directive 2010/63/EU of the European parliament and of the council of 22 September 2010 on the protection of animals used for scientific purposes. Off J Eur Union. 2010;27633.
10 Perrée J, Van Leeuwen TG, Kerindongo R, Spaan JAE, VanBavel E. Function and structure of pressurized and perfused porcine carotid arteries: effects of in vitro balloon angioplasty. Am J Pathol. 2003;163(5):1743–50.
11 Mattsson E, Brunkwall J, Bergqvist D. Influence of transluminal angioplasty on the prostanoid release from the arterial wall. Eur J Vasc Surg. 1990;4(1):11–7.
12 Fischell TA, Grant G, Johnson DE. Determinants of smooth muscle injury during balloon angioplasty. Circulation. 1990 Dec;82(6):2170–84.
13 Cunningham KS, Gotlieb AI. The role of shear stress in the pathogenesis of atherosclerosis. Lab Invest. 2005 Jan;85(1):9–23.
14 Pietersma A, Kofflard M, de Wit LE, Stijnen T, Koster JF, Serruys PW, et al. Late lumen loss after coronary angioplasty is associated with the activation status of circulating phagocytes before treatment. Circulation. 1995 Mar;91(5):1320–5.
15 Hamza LH, Dang Q, Lu X, Mian A, Molloi S, Kassab GS. Effect of passive myocardium on the compliance of porcine coronary arteries. Am J Physiol Heart Circ Physiol. 2003 Aug;285(2):H653–60.
16 Kelly RF, Snow HM. The effect of arterial wall shear stress on the incremental elasticity of a conduit artery. Acta Physiol. 2011 May;202(1):1–9.
17 Yao L, Xue X, Yu P, Ni Y, Chen F. Evans blue dye: a revisit of its applications in biomedicine. Contrast Media Mol Imaging. 2018;2018:1–10.
18 Autar A, Taha A, van Duin R, Krabbendam-Peters I, Duncker DJ, Zijlstra F, et al. Endovascular procedures cause transient endothelial injury but do not disrupt mature neointima in Drug Eluting Stents. Sci Rep. 2020;10(1):2173–8.
19 Woolf MS, Dignan LM, Scott AT, Landers JP. Digital postprocessing and image segmentation for objective analysis of colorimetric reactions. Nat Protoc. 2021 Jan 9;16(1):218–38.
20 Saad HA, Terry MA, Shamie N, Chen ES, Friend DF, Holiman JD, et al. An easy and inexpensive method for quantitative analysis of endothelial damage by using vital dye staining and adobe photoshop software. Cornea. 2008;27(7):818–24.
21 Nakladal D, Buikema H, Romero AR, Lambooy SPH, Bouma J, Krenning G, et al. The (R)-enantiomer of the 6-chromanol derivate SUL-121 improves renal graft perfusion via antagonism of the α1-adrenoceptor. Sci Rep. 2019;9(1):13.
22 Rees DD, Palmer RMJ, Hodson HF, Moncada S. A specific inhibitor of nitric oxide formation from l-arginine attenuates endothelium-dependent relaxation. Br J Pharmacol. 1989;96(2):418–24.
23 Miyata K, Shimokawa H, Yamawaki T, Kunihiro I, Zhou X, Higo T, et al. Endothelial vasodilator function is preserved at the spastic/inflammatory coronary lesions in pigs. Circulation. 1999;100(13):1432–7.
24 Nandan S, Schiavi-Tritz J, Hellmuth R, Dunlop C, Vaughan TJ, Dolan EB. Design and verification of a novel perfusion bioreactor to evaluate the performance of a self-expanding stent for peripheral artery applications. Front Med Technol. 2022;4(June);4:886458.
25 Koo Y, Tiasha T, Shanov VN, Yun Y. Expandable Mg-based helical stent assessment using static, dynamic, and porcine ex vivo models. Sci Rep. 2017;7(1):1173–10.
26 Udofot O, Lin LH, Thiel WH, Erwin M, Turner E, Miller FJ, et al. Delivery of cell-specific aptamers to the arterial wall with an occlusion perfusion catheter. Mol Ther Nucleic Acids. 2019 June 16;16:360–6.
27 Lignell S, Lohmann S, Rozenberg KM, Leuvenink HGD, Pool MBF, Lewis KR, et al. Improved normothermic machine perfusion after short oxygenated hypothermic machine perfusion of ischemically injured porcine kidneys. Transpl direct. 2021 Feb;7(2):e653.
28 Bardy N, Karillon GJ, Merval R, Samuel JL, Tedgui A. Differential effects of pressure and flow on DNA and protein synthesis and on fibronectin expression by arteries in a novel organ culture system. Circ Res. 1995 Oct;77(4):684–94.
29 Consigny PM, Tulenko TN, Nicosia RF. Immediate and long-term effects of angioplasty-balloon dilation on normal rabbit iliac artery. Arteriosclerosis. 1986;6(3):265–76.
30 Fischell TA, Nellessen U, Johnson DE, Ginsburg R. Endothelium-dependent arterial vasoconstriction after balloon angioplasty. Circulation. 1989;79(4):899–910.
31 Russo RJ, Silva PD, Yeager M. Coronary artery overexpansion increases neointimal hyperplasia after stent placement in a porcine model. Heart. 2007;93(12):1609–15.
32 Lu X, Kassab GS. Nitric oxide is significantly reduced in ex vivo porcine arteries during reverse flow because of increased superoxide production. J Physiol. 2004 Dec;561(Pt 2):575–82.